

A FRACTURE FAILURE CRITERION FOR CONCRETE-CONCRETE INTERFACE UNDER MIXED MODE LOADING CONDITION

ZEESHAN ABBAS* AND K. M. PERVAIZ FATHIMA[†]

Indian Institute of Technology
Jammu, J&K India

*e-mail: zeeshan.abbas@iitjammu.ac.in

[†]e-mail: pervaiz.khatoon@iitjammu.ac.in

Key words: Concrete-concrete interface, Failure pattern, Acoustic emission, mode mixity

Abstract. Various important concrete structures are susceptible to imperfections, such as the presence of an interface. In some cases, the formation of an interface is an inevitable flaw, such as in the case of repair, dams and pre-cast concrete structures. These flaws can act as a weak link and could be responsible for the failure of the structures. One of the most widely used nondestructive techniques to monitor such damages in structures in real time is the acoustic emission (AE) technique. In this study, experimental tests are conducted on concrete-concrete interface specimens under four-point shear tests with different interface positions. The interfaces are formed between four different strengths of concrete on each side. The AE technique is used to monitor the crack growth. Based on the experimental results, A fracture criterion has been suggested based on simplified calculation of mode mixity ratio. Three different failure patterns have been identified depending on the mode mixity ratio, where cracks eventually kinked into the substrate material at a critical value of the mode mixity ratio.

1 INTRODUCTION

Concrete–concrete interface is seen in all sorts of civil engineering construction elements such as buildings, bridges, pavements, dams, and tunnels. The presence of an interface may be accidental due to poor management, or its presence can be inevitable as in case of a mass concreting structures such as a tunnel lining or a dam. An interface may form as a result of a technique to strengthen or repair an existing structure, where a fresh layer of concrete is cast over old concrete or it may even be formed during the construction of new structural elements, such as between precast components and cast-in-place elements. The material discontinuity, accumulation of pores and the concentration of micro-cracks at an interface makes it the weakest link in a concrete composite [3]. The bond strength at the concrete–concrete interface

must be sufficient in order to effectively transfer load between two components, thus achieving a monolithic behaviour.

Kishen and Rao [6] studied fracture at a cold joint in concrete by varying the grades of concrete on either side of interface and concluded that greater the difference in strengths poorer the repair mechanism. Geometrically similar specimens with transverse cold joints were studied under both static and fatigue loading [9]. Koh et al. [7] proposed a way to evaluate the serviceability of reinforced concrete T-girder when subjected to carbonation taking in to account the cold joints and loading effects. A recent case study points out the extent to which cold joints influence the serviceability of tunnel linings [1]. Fu et al. [2] studied the fracture at a concrete-concrete interface formed by varying the pouring intervals under three point bend

test.

The fracture at a bi-material interface is governed by the mode mixity $\psi = K_{II}/K_I$ ratio [4]. Most of the available work on concrete-concrete interface only accounts for mode I loading conditions. This study attempts to get a broad range of mode mixity by varying the loading condition at the initial crack tip present along the interface and study the failure pattern as loading changes from pure mode I to mode II. Also the samples while loading are monitored by acoustic emission (AE) technique. The application of AE parameters such as energy are used to further analyze the fracture process in concrete-concrete interface.

2 Experimental Program

2.1 Design of specimen

Four different mixes of concrete are designed namely A, B, C and D. Keeping mix A as a primary or the old set, mix B, C and D are cast as a new material against mix A. The size of the interface beams are 500 mm \times 100 mm \times 100 mm. The span is kept 400 mm. The notch to depth ratio is kept 0.3. A broad range of ψ can be observed by varying the length of mix A portion L_r of the beam see Figure 1, four combinations have been cast viz. AA, AB, AC and AD. For each mix combination, the length L_r is set so that four different eccentricity values e of the interface from the center of the beam are obtained i.e. 00 mm, 12 mm, 24 mm and 36 mm. For each e considered, three sets of specimens are fabricated. The specimens are fabricated by casting the first half of the beam on day one to the appropriate lengths L_r . On day two surface is cleaned and a PVC plate is pasted at the place of notch and the second half of the beam is cast. The specimens are kept for curing in water for 28 days before testing. To compute the material properties, intact beams of size 500 mm \times 100 mm \times 100 mm are cast along with cylinders of diameter 150 mm and depth 300 mm.

2.2 Material properties

To compute the Poisson's ratio and Young's modulus cylinders are tested using compression

testing machine. Three point bend test is conducted on intact beams using RILEM standard [8] and accordingly fracture energy has been calculated for each mix as given in Table 1.

2.3 Four point shear (FPS) test

A 350 kN servo controlled testing machine is used for the FPS tests. The proportion of loads on the two loading points is 1:4. The crack mouth opening displacement (CMOD), the crack mouth sliding displacement (CMSD) and load point displacement are measured using clip gauge and linear variable displacement transducers (lvdt). The schematic experimental setup for the FPS test is shown in Figure 1. The beams are tested under CMOD control with a loading rate of 0.024 mm/min.

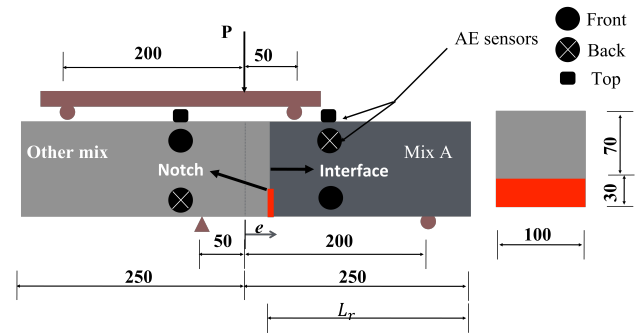


Figure 1: Schematic diagram of the FPS test

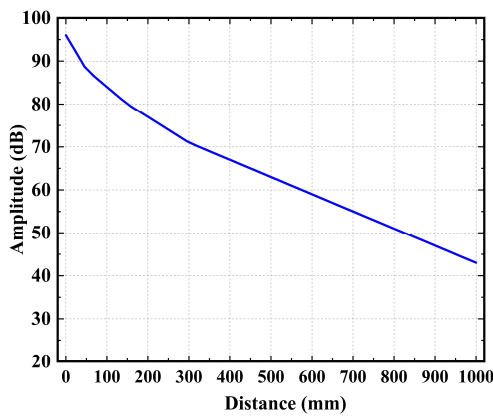
2.4 Acoustic emission

The AE signal is acquired by means of 6 piezo electric sensors (type: R6I-AST, built-in 40 dB preamplifier), and background noise threshold was set at 38 dB. Peak definition time (PDT), hit definition time (HDT) and hit lock-out time (HLT) were set to 50 μ s, 150 μ s and 300 μ s respectively. Sampling rate set to 1 MHz. A pencil lead break test was performed, where two sensors were placed at various known locations and a pencil lead was broken to mimic a real crack, The distance between the sensors divided by the difference in arrival time of the signal at each sensors gives us the P wave velocity for the material. Furthermore, an Acoustic Property Matrix Generator (APMG) feature available in AE win software is utilised to verify

Table 1: Material properties

| Designation | Characteristic strength (MPa) | Poissons' ratio | E (GPa) | P_{max} (kN) | G_F (N/m) |
|-------------|-------------------------------|-----------------|---------|----------------|-------------|
| A | 35 | 0.200 | 29.6 | 4.00 | 122.80 |
| B | 30 | 0.210 | 27.4 | 3.70 | 117.22 |
| C | 40 | 0.195 | 31.6 | 4.60 | 144.90 |
| D | 45 | 0.190 | 33.5 | 5.09 | 148.57 |

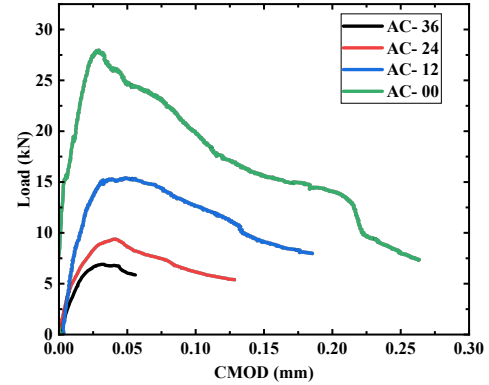
the same and also find the attenuation of amplitude when a signal passes through the material shown in Figure 2.

**Figure 2:** Acoustic signal attenuation curve

3 Experimental results

The experimental program results consist of the specimens' loading responses, including P-CMOD curves, the maximum load (P_{max}), and the failure modes of each specimen. In addition to that, Acoustic emission results in terms of cumulative energy and AE events are also presented.

Figure 3 shows the load-CMOD curve for combination AC. It can be seen that for greater mode mixity i.e. smaller value of e the fracture energy is relatively more. The highest is for pure mode II i.e. when $e = 0$ mm. Similar pattern could be seen in other combinations as well. Not just the fracture energy the failure modes also vary, as we move from lower to higher e which will be discussed in subsequent sections.

**Figure 3:** P-CMOD curves for different e for mix combination AC

3.1 Failure Modes

Three different types of failure modes are observed during the four point shear test of interfacial beams. Based on the proportion of shear to tensile loading at the interface, crack propagation pattern changes and are being discussed here.

1. Interface failure along the concrete-concrete interface (I).

Figure 4 shows I type failure mode. Mostly this type of failure mode is expected in specimens with larger e viz $e = 26$ mm - 38 mm. In these specimens, the proportion of Mode II to Mode I type of loading i.e. mode mixity is less. In other words the proportion of shear to tensile loading is less. Therefore, the crack propagates through the concrete-concrete interface up to failure

2. Kinking of interface crack into the substrate (K).

Figure 5 displays an example of this type of failure mode, which is mostly expected

in specimens with relatively small values of $e = 0$ mm to 12 mm. In these specimens, the normal stresses at the position of concrete–concrete interface is lesser in comparison to earlier case. Therefore, the proportion of the shear stress to tensile stress is relatively more i.e. relatively higher mode mixity. In this failure mode the crack initially propagates through the weak interface and then it deviates into one of the substrates until failure.



Figure 4: Interface failure



Figure 5: Interface cracking and kinking

3. Kinking of interface crack into the substrate followed by brittle failure (KB)

This failure mode could be seen in specimens with $e = 0$ mm shown in Figure 6. In these specimens, the crack initiated through the interface and kinked in to the substrate. As the crack advanced towards the top face of the beam, a secondary crack initiates close to the concrete support, which is then followed by a brittle failure. In this case the mode mixity is highest as the proportion of mode

II to mode I loading at the interface is highest. The magnitude of bending moment in this case approaches to almost zero. A fair inference for this type of failure could be that when the mode mixity is higher than a certain critical value, the strength of the interface seem to be relatively closer to strength of either material. This type of failure where beam fails at the loading point resembles a typical four point bending test [5].

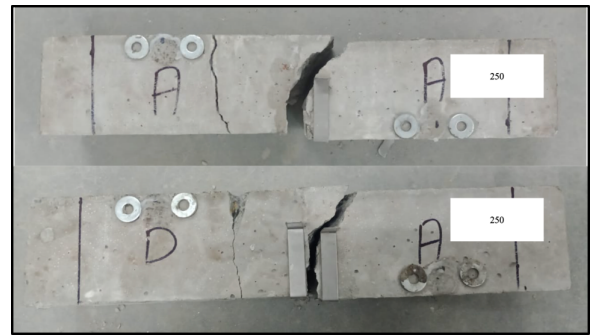


Figure 6: Interface cracking, kinking and brittle failure at load point

3.2 Failure criterion

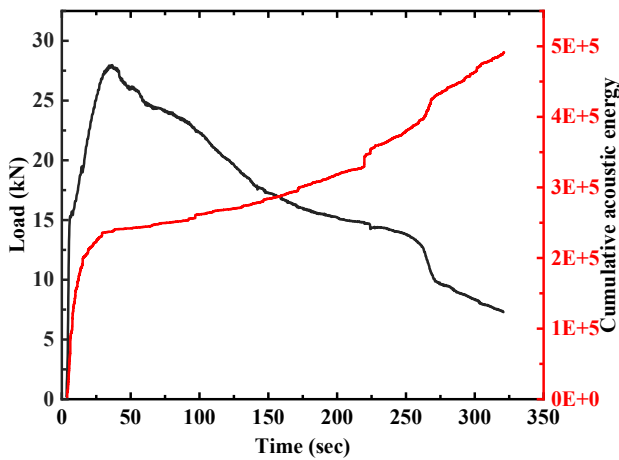
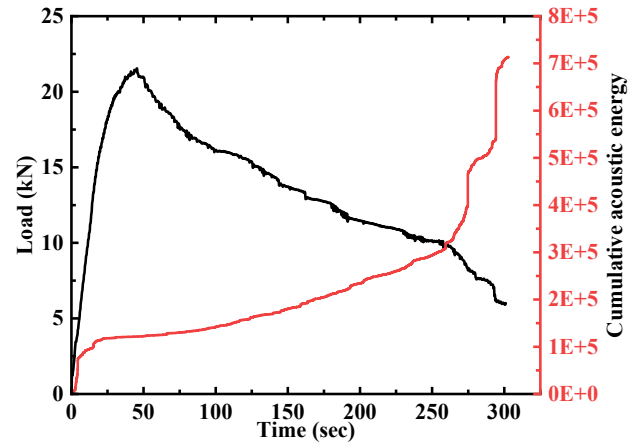
The experimental results enabled the exploration of effect of mode mixity ratio. In this study mode mixity ratio is simplified in terms of proportion of shear to normal stress proportion and represented as $\phi = \frac{\tau}{\sigma}$ not to be mistaken with actual mode mixity ratio ψ . With in the scope of this paper we have a simplified ratio to represent the proportion of mode I and mode II condition. The ratio ϕ ranges from 2.1 to 61 for study as illustrated in Table 2. Based on the observed behaviour corresponding to the failure pattern a failure criterion could be developed as $\phi < 8.8$ crack tends to follow the interface and $\phi > 8.8$ crack tends to kink and for even higher value of phi a secondary brittle crack forms and propagates at the loading point.

Table 2: Failure mode and simplified mode mixity ratio

| e | ϕ | Failure mode |
|-----|--------|-----------------------|
| 00 | 61.25 | K / KB (Figures 5, 6) |
| 12 | 8.82 | K (Figure 5) |
| 24 | 4.72 | Mode I (Figure 4) |
| 36 | 2.17 | Mode I (Figure 4) |

3.3 Acoustic emission

Acoustic emission energy is the energy under the waveform envelop. The cumulative AE energy as a function of time is plot in Figure 8 and 7. Figure 7 is a typical representation of AE energy release for a cases I and K, the initial rise in AE energy before reaching the peak load, indicating the formation of micro-cracks in a short interval of time. At this stage, First macro crack initiates and is associated with a higher energy release rate. The subsequent flat portion typically corresponds to the propagation of macro-cracks, generally characterised by a lower energy release rate. Sudden jumps in AE energy are attributed to the coalescence of micro cracks. Figure 8 is representation of AE energy release for case KB, a steep increase in energy release rate can be observed around 270 seconds, which corresponds to the formation of a secondary crack at the loading point, which is abrupt and brittle in nature.


Figure 7: Representation of cumulative AE energy vs time on load-time graph failure I and K

Figure 8: Representation of cumulative AE energy vs time on load-time graph for failure KB

4 Conclusions

In this study, the effect of varying mode mixity ratio ϕ on the fracture behavior of concrete–concrete interface crack has been investigated. FPS tests are performed on concrete–concrete interfacial beams. In order to capture the acoustic response during the test AE sensors are attached to the specimen. The experimental program is designed so that a broad range of ϕ can be tested. The following conclusions are drawn:

- The simplified mode mixity ratio ϕ affects the failure mode at a concrete–concrete interface. The specimen with lower mode mixity ratio fails by cracking through the interface while for a specimen with higher mode mixity ratio crack deviates into one of the material.
- The fracture energy of concrete–concrete interface beam which is the area under the load-CMOD curve increases with increase in mode mixity ratio, reason being for higher mode mixity ratio the load carrying capacity as well as the ductility seem to increase.

Acknowledgement

The authors gratefully acknowledge the financial support from SERB-DST, Government of India.

References

- [1] Fu, H.-L., Deng, H.-S., Shi, Y., Wu, Y.-M. and Zhao, Y.-B. [2024], 'Analysis method for cracking and safety status of plain concrete lining with cold joints', *Case Studies in Construction Materials* **21**, e03696.
- [2] Fu, H.-L., Deng, H.-S., Zhang, J., Shi, Y. and Huang, X. [2022], 'Experimental analysis of influence of pouring interval on fracture performance of concrete structures with cold joints', *Theoretical and Applied Fracture Mechanics* **118**, 103289.
- [3] He, Y., Zhang, X., Hooton, R. and Zhang, X. [2017], 'Effects of interface roughness and interface adhesion on new-to-old concrete bonding', *Construction and Building Materials* **151**, 582–590.
- [4] Hutchinson, J. and Suo, Z. [1991], 'Mixed mode cracking in layered materials', *Advances in Applied Mechanics* **29**, 63–191.
- [5] Indian Standards Institution [1959], 'IS 516:1959 - Method of Tests for Strength of Concrete', Bureau of Indian Standards, New Delhi. Reaffirmed in 2002.
- [6] Kishen, J. C. and Rao, P. S. [2007], 'Fracture of cold jointed concrete interfaces', *Engineering fracture mechanics* **74**(1-2), 122–131.
- [7] Koh, T.-H., Kim, M.-K., Yang, K.-H., Yoon, Y.-S. and Kwon, S.-J. [2019], 'Service life evaluation of rc t-girder under carbonation considering cold joint and loading effects', *Construction and Building Materials* **226**, 106–116.
- [8] RILEM 50-FMC Draft Recommendation [1985], 'Determination of the fracture energy of mortar and concrete by means of three-point bend tests on notched beams', *Materials and Structures* **18**(4), 287–290.
- [9] Shah, S. G., Ray, S. and Kishen, J. C. [2014], 'Fatigue crack propagation at concrete–concrete bi-material interfaces', *International journal of fatigue* **63**, 118–126.